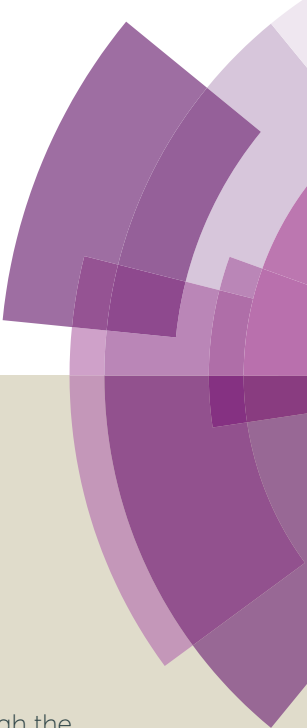


Chemical Science

Accepted Manuscript



This is an Accepted Manuscript, which has been through the Royal Society of Chemistry peer review process and has been accepted for publication.

Accepted Manuscripts are published online shortly after acceptance, before technical editing, formatting and proof reading. Using this free service, authors can make their results available to the community, in citable form, before we publish the edited article. We will replace this Accepted Manuscript with the edited and formatted Advance Article as soon as it is available.

You can find more information about Accepted Manuscripts in the [Information for Authors](#).

Please note that technical editing may introduce minor changes to the text and/or graphics, which may alter content. The journal's standard [Terms & Conditions](#) and the [Ethical guidelines](#) still apply. In no event shall the Royal Society of Chemistry be held responsible for any errors or omissions in this Accepted Manuscript or any consequences arising from the use of any information it contains.

Synthesis of Yellow and Red Fluorescent 1,3a,6a-Triazapentalene and Theoretical Investigation of Optical Properties

Cite this: DOI: 10.1039/xoxxxxxxx

Received 00th January 2012,
Accepted 00th January 2012

DOI: 10.1039/xoxxxxxxx

www.rsc.org/

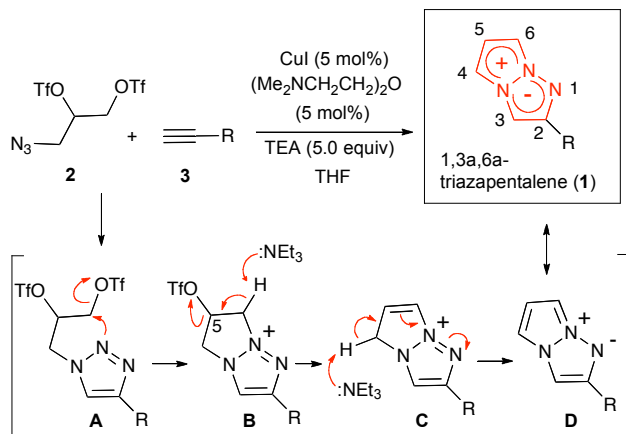
Kosuke Namba^{a*}, Ayumi Osawa^b, Akira Nakayama^{d*}, Akane Mera^b, Fumi Tano^b, Yoshiro Chuman^c, Eri Sakuda^c, Tetsuya Taketsugu^c, Kazuyasu Sakaguchi^c, Noboru Kitamura^c, and Kei Tanino^{c*}

To expand the originally developed fluorescent 1,3a,6a-triazapentalenes as fluorescent labeling reagents, the fluorescence wavelength of 1,3a,6a-triazapentalene was extended to the red color region. Based on the noteworthy correlation of the fluorescence wavelength with the inductive effect of the 2-substituent, further electron-deficient 2-(2-cyano-4-methoxycarbonylphenyl)-1,3a,6a-triazapentalene and 2-(2,6-dicyano-4-methoxycarbonylphenyl)-1,3a,6a-triazapentalene were synthesized. The former exhibited yellow and the latter exhibited red fluorescence, and both compounds exhibited large Stokes shifts, and the 1,3a,6a-triazapentalene system enabled the same fluorescent chromophore to cover the entire region of visible wavelengths. The potential applications of the 1,3a,6a-triazapentalenes as fluorescent probes in the fields of the life sciences were investigated, and the 1,3a,6a-triazapentalene system was clearly proven to be useful as a fluorescent reagent for live cell imaging. Quantum chemical calculations were performed to investigate the optical properties of 1,3a,6a-triazapentalenes. These calculations revealed that the excitation involves a significant charge-transfer from the 1,3a,6a-triazapentalene skeleton to the 2-substituent. The calculated absorption and fluorescence wavelengths showed a good correlation with the experimental ones, and thus the system would enable the theoretical design of substituents with the desired optical properties.

Introduction

Fluorescent organic molecules are an important class of compounds in modern science and technology, and are widely used as biological imaging probes, sensors, lasers, and light-emitting devices.¹ Thus, the development of useful fluorescent organic molecules is crucial for the advancement of many industries, and has been a subject of intensive research.² In particular, small fluorescent organic molecules have attracted great attention in a chemical biology field, because visualization of biologically active small compounds by introducing fluorophores is one of the most useful way for their mechanistic study.³ However, several key improvements are needed for the commonly used fluorescent molecules. Most highly fluorescent molecules possess relatively large molecular sizes depending on the target bioactive compounds, and the fluorescence labeled molecules sometimes lost their activities as a result of the structural modifications. Furthermore, often the methods used to synthesize them do not allow the design of systems whose luminescent properties span a wide range of wavelengths. As a potential fluorescent chromophore to overcome the above problems, we have recently discovered that a 1,3a,6a-triazapentalene skeleton without an additional fused ring system is a compact and highly fluorescent chromophore.^{4,5} In contrast, benzotriazapentalene as an aryl fused ring system exhibits almost no fluorescence ($\Phi_F <$

0.001),⁶ and the various related analogues of aryl fused 1,3a,6a-triazapentalenes⁷ have not been reported to have noteworthy fluorescence properties. The limited synthesis of 1,3a,6a-triazapentalenes without an aryl fused system⁸ might be the main reason that they have been previously unrecognized as an excellent fluorescent chromophore until our finding.



Scheme 1 Single Step Synthesis of 1,3a,6a-triazapentalenes (1).

Construction of 1,3a,6a-triazapentalene skeleton without an aryl fused ring system was recently established in our laboratory, and 1,3a,6a-triazapentalenes are readily prepared by

ARTICLE

Journal Name

the click-cyclization-aromatization cascade reaction of various alkynes with the azide **2** possessing two triflates at each of the C2 and C3 positions (Scheme 1).⁴ The click reaction of azide **2** with alkynes afforded a triazole **A**, which underwent cyclization to give a triazolium ion **B**. In the presence of triethylamine, the intermediate **B** was subsequently converted to triazapentalene **1** by a sequential reaction of E2 elimination and deprotonation (Scheme 1). This cascade reaction was confirmed to be applicable to a wide range of alkynes, and the easy access to the various 1,3a,6a-triazapentalenes was enabled. Furthermore, the 5,5-dimethoxy analog of **B** was found to be stable enough for isolation, and a strong base was necessary for elimination of the methoxy group to give 5-methoxy-1,3a,6a-triazapentalenes. This method was applicable to the one-pot synthesis of the various 2,5-disubstituted-1,3a,6a-triazapentalenes.⁹ Although the 1,3a,6a-triazapentalenes are composed of zwitter ion, the polarities and the electrical charges are neutral due to the resonance stabilization as the aromatic compounds so that they are easily manipulated.

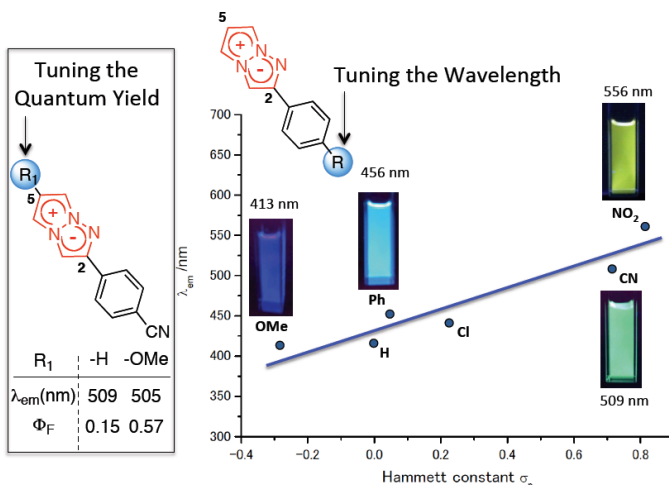


Figure 1 Substitution Effect on Fluorescence Properties of 1,3a,6a-Triazapentalenes. The values determined in deaerated dichloromethane.

The 1,3a,6a-triazapentalenes exhibit not only intense fluorescence but also various interesting fluorescence properties such as an extremely large Stokes shift (Stokes shift exceeding 100 nm)¹⁰ and large positive fluorescence solvatochromism. More interestingly, the 1,3a,6a-triazapentalenes as fluorescent chromophores provide an innovative fluorescence system that can tune both the fluorescence wavelength and quantum yield by the 2- and 5-substituents, respectively.^{4,9} For example, the fluorescence of the 1,3a,6a-triazapentalenes shifted to longer wavelengths along with the inductive effect of the 2-substituents. In fact, the fluorescence maxima of the 2-phenyl-1,3a,6a-triazapentalene derivatives exhibited a noteworthy correlation with the Hammett σ_p value of the substituent on the benzene ring, as shown in Figure 1. In contrast, the introduction of an electron donating substituent at the C5 position had little effect on the fluorescence wavelength, although the enhancement of the push-pull effect on the 10 π -electron system was expected. Meanwhile, the fluorescence quantum yields

(Φ_F) were dramatically changed. In fact, the introduction of a methoxy group at the C5 position of 2-(4-cyanophenyl)-1,3a,6a-triazapentalene allowed a substantial increase in Φ_F (from 0.15 to 0.57) without any effect on the fluorescence wavelength.

Recently, emission and/or quantum yields tunable fluorophores have been received a great deal of attention as a core skeleton of fluorescent probes.¹¹ The 1,3a,6a-triazapentalene system also provides a novel fluorescent molecule that enables the same fluorescent chromophore to exhibit various fluorescence colors and quantum yields. However, the detailed mechanisms of the above interesting fluorescence properties have not been elucidated.

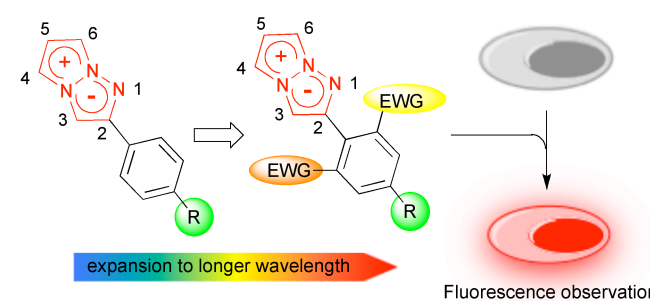


Figure 2 Design of Yellow and Orange Fluorescent 1,3a,6a-Triazapentalene and Its Application to Cell Staining

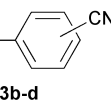
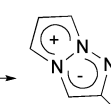
To actually develop the 1,3a,6a-triazapentalenes as fluorescent labeling reagents, several goals had to be met: (i) the expansion of the fluorescence wavelength of triazapentalenes to the red color region, (ii) the confirmation that the fluorescence of triazapentalene from the inside of cells is observable, (iii) the introduction of binding sites such as succinimide ester and a maleimide as labeling reagents, and (iv) the theoretical explanation of the fluorescence properties of 1,3a,6a-triazapentalene. The fluorescent labels exhibiting longer emission wavelengths, such as those emitting yellow, orange, and red light, might be more suitable for the living cells and tissues due to the reduction of the light irradiation damage and the potential access to deeper tissue. However, the existing fluorescence organic molecules emitting red light have several common problems, including large molecular size and small Stokes shift.^{11,12} On the other hand, the 1,3a,6a-triazapentalene is a compact fluorescent chromophore exhibiting a large Stokes shift, and its fluorescence wavelength can be tuned based on the inductive effect of C2-substituents. Although the fluorescence wavelengths of the 1,3a,6a-triazapentalene derivatives previously reported in a preliminary communication are below the 556 nm (lime green) wavelength of 2-(4-nitrophenyl)-1,3a,6a-triazapentalene, additional introductions of electron-withdrawing groups on the benzene ring are expected to induce additional and longer wavelength shifts. Thus, we became intrigued with the synthesis of 1,3a,6a-triazapentalenes possessing additional electron-withdrawing groups in order to elucidate the possibility of 1,3a,6a-triazapentalenes emitting yellow, orange, and red light. Herein, we describe the synthesis

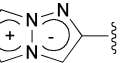
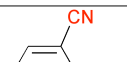
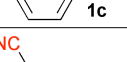
of 2-phenyl-1,3a,6a-triazapentalene derivatives possessing both electron-withdrawing groups and binding sites on the benzene ring, the observance of their fluorescence inside cells, and the computational efforts made to provide a theoretical explanation of the fluorescence properties of 1,3a,6a-triazapentalenes.

Results and Discussion on Synthesis and Fluorescence Properties

A cyano group was chosen as the electron-withdrawing group due to its small size and excellent stability against UV irradiation. Thus, a suitable position for introduction of the cyano group to the benzene ring was first investigated. Treatments of **2** with the phenyl acetylene derivatives possessing a cyano group at para **3b**, meta **3c**, and ortho position **3d** in the presence of the CuI•ligand complex and triethylamine gave the desired triazapentalenes **1b**, **1c**, and **1d** in 77%, 87%, and 93% yields, respectively (Table 1).

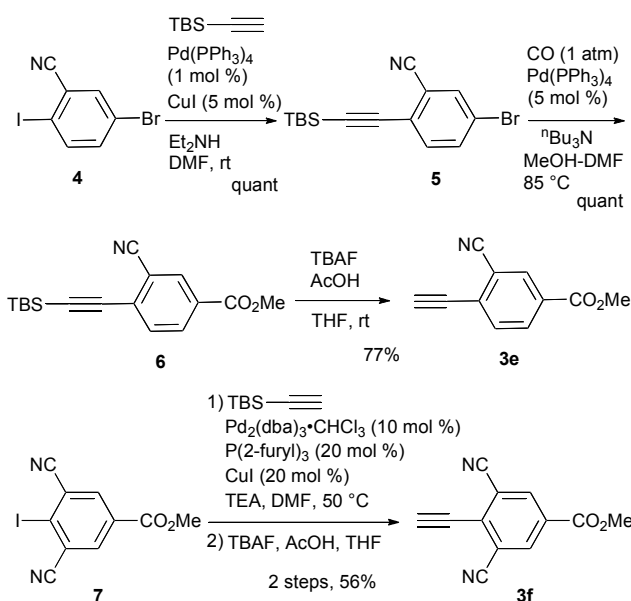
Table 1 Orientational Effects of the Cyano Group on the Benzene Ring in Degerated Dichloromethane

		CuI (5 mol%) (Me ₂ NCH ₂ CH ₂) ₂ O (5 mol%)	TEA (5.0 equiv) THF (0.01 M)	1b-d
2	+ 			
(1.2 equiv)				

	yield (%)	$\lambda_{\text{abs}}^{\text{max}}$ (nm)	$\lambda_{\text{em}}^{\text{max}}$ (nm)	Φ_F	color
 1b	77	381	509	0.15	
 1c	87	327	493	0.24	
 1d	93	376	515	0.24	

In comparison with para-substituent **1b**, the introduction of a cyano group at meta position (**1c**) induced the undesired shorter wavelength shift, although the Φ_F value was increased to 0.24 (Table 1).¹³ In contrast, the ortho-cyano analog **1d** exhibited a slight longer-wavelength shift, and the Φ_F value was also increased (Table 1).¹³ Therefore, we found that the ortho positions are more suitable for introduction of the cyano group as an additional electron-withdrawing group for expansion of the fluorescence wavelength to the yellow and red color region. Thus, we first tried to synthesize the methyl 3-cyano-4-ethynylbenzoate **3e** as an alkyne fragment. The commercially available 5-bromo-2-iodobenzonitrile **4** was converted into ethynylbenzonitrile **5** by the Sonogashira coupling reaction with *tert*-butyldimethylsilylacetylene.¹⁴ Treatment of **5** with 5 mol% of Pd(PPh₃)₄ in methanol under a CO atmosphere

afforded methyl ester **6** in quantitative yield. Finally, removal of the TBS group gave the desired alkyne fragment **3e** (Scheme 2). Next, we tried to synthesize the dicyano analog, which was expected to induce a further wavelength shift. The 3,5-dicyano-4-iodo-benzoate **7** as a starting material was obtained from the commercially available *p*-toluidine in 5 steps according to the procedure of Professor Gübel.¹⁵ The Sonogashira coupling reaction of **7** with various acetylenes was initially difficult, and yielded mainly the deiodinated reductive product.¹⁶ After various examinations, we found that the reaction with TBS-acetylene under the condition of 10 mol % of Pd₂(dba)₃•CHCl₃, 20 mol % of trifurylphosphine, 20 mol % of copper(I) iodide, and triethylamine in DMF at 50 °C afforded the desired coupling product. Finally, subsequent treatment with TBAF and acetic acid gave the alkyne fragment **3f**.



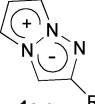
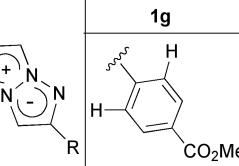
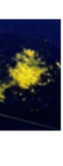
Scheme 2 Synthesis of Alkyne Fragment **3e** and **3f**

Next, the cascade reaction leading to 1,3a,6a-triazapentalenes was applied to the prepared alkynes **3e** and **3f**. Treatment of **3e** with 1.2 equiv of **2** in the presence of 5 mol % of the CuI•ligand complex and triethylamine afforded the desired 1,3a,6a-triazapentalene **1e** in 71% yield. The similar click reaction of **3f** also smoothly proceeded to give **1f** in 72% yield. Furthermore, the comparative analog **1g**, which did not possess cyano groups, was also synthesized in 73% yield from methyl 4-ethynylbenzoate (**3g**). Having prepared the desired 1,3a,6a-triazapentalenes **1e**, **1f**, and **1g**, their fluorescence properties were examined (Table 2). Since these three compounds were slightly soluble in water due to the lipophilicity of the benzene ring, their fluorescence spectra were measured in deaerated dichloromethane. The standard analog **1g** exhibited a high fluorescence quantum yield ($\Phi_F = 0.44$)¹³ and green emission ($\lambda_{\text{em}}^{\text{max}} = 510 \text{ nm}$) as predicted from the Hammett σ_p value of methyl ester on the benzene ring. As we expected, the mono-cyano analog **1e** showed a noteworthy longer-wavelength shift of the fluorescence

maximum from 510 nm of **1g** to 572 nm, and **1e** emitted yellow light. Although the fluorescence quantum yield (Φ_F) of **1e** was slightly decreased to 0.34,¹⁷ this value was still within the range of an effective fluorescent labeling reagent. Furthermore, the fluorescence maximum of the di-cyano analog **1f** shifted to a still longer-wavelength region (632 nm), and **1f** showed red fluorescence. Therefore, the introductions of the cyano groups were found to induce an approximately 60 nm longer shift of the fluorescence maximum in each case, and the development of yellow and red fluorescent 1,3a,6a-triazapentalenes was accomplished.

It was especially noteworthy that these long-wavelength fluorescent molecules exhibited large Stokes shifts, such as the 152 nm shift of **1e** and 166 nm shift of **1f**, despite there having been few prior examples of the long-wave (> 550 nm) organic fluorophores exhibiting such large (mega) Stokes shifts,¹⁸ since such shifts were useful for suppressing the action of background fluorescence in the various fluorescent analyses. In addition, the molecular sizes of **1e** and **1f** were considerably small in comparison with the conventional yellow and red fluorescent molecules. Therefore, the 1,3a,6a-triazapentalenes might be practical fluorescent chromophores for use as molecular probes to cover the entire region of visible wavelengths, although the further shift toward longer wavelengths is still needed. Furthermore, **1g** and **1e** showed fluorescence emission in the solid state with a fluorescence maximum similar to the solution of dichloromethane, whereas the fluorescence of **1f** in the solid state was not detected.

Table 2 Yields and Fluorescence Properties of **1g**, **1e**, and **1f**

			CuI (5 mol%)	(Me ₂ NCH ₂ CH ₂) ₂ O (5 mol%)	
	2 (1.2 equiv)	3e-g		TEA (5.0 equiv)	
1g					
					
yield	73%		71%		72%
$\lambda_{\text{abs}}^{\text{max}}$ (nm)	solution ^a	solid	solution ^a	solid	solution ^a
$\lambda_{\text{em}}^{\text{max}}$ (nm)	376	N/A	420	N/A	466
Φ_F	0.44	0.06	0.34	0.06	0.096
color					

^ain deaerated dichloromethane

On the other hand, the extinction coefficient (ϵ) of **1g** at 376 nm was $1230 \text{ dm}^3 \text{ mol}^{-1} \text{ cm}^{-1}$, and this value was still needed to increase for more brightly fluorescent reagent. Although the ϵ value at 287 nm was $13800 \text{ dm}^3 \text{ mol}^{-1} \text{ cm}^{-1}$ as a practical level, this region (ultraviolet) is not suitable as an excitation light for imaging probes. Similarly, the extinction coefficients (ϵ) of **1e** and **1f** in a visible light region were also not high as $630 \text{ dm}^3 \text{ mol}^{-1} \text{ cm}^{-1}$ (420 nm) and $1580 \text{ dm}^3 \text{ mol}^{-1} \text{ cm}^{-1}$ (466 nm), respectively. Therefore, improvement of the extinction coefficient (ϵ) was the next challenge for the more useful bright fluorescent labels. So far, we have already found that the introduction of a substituent at the C4 position dramatically increases the ϵ value. For example, 4-phenyl analogs of **1g** showed a substantial increase in ϵ from $1230 \text{ dm}^3 \text{ mol}^{-1} \text{ cm}^{-1}$ (376 nm) of **1g** to 22600 (345 nm) with comparable Φ_F . The 4-phenyl analog of **1e** also exhibited a practical value of ϵ as 4560 (432 nm) and 38000 (336 nm), although the Φ_F value was decreased to 0.07.¹⁹ Further investigation of 4-substituents for the practical fluorescent labeling reagent is currently underway in our laboratory.

Furthermore, fluorescence solvatochromism of **1e** was examined. The fluorescence spectra of **1e** in several solvents are shown in Figure 3. Basically, the fluorescence from **1e** shifted to the longer wavelength with the Stokes shift being increased by an increase in the solvent polarity from benzene (545 nm) to acetone (645 nm). On the other hand, the fluorescence in methanol shifted inversely to the shorter wavelength ($\lambda_{\text{em}}^{\text{max}} = 463$ nm). Furthermore, since **1e** was slightly soluble in water, a supernatant solution was measured. The fluorescence shifted to 476 nm in a similar behavior to methanol. The fluorescence quantum yield in water substantially decreased to 0.013. Therefore, 1,3a,6a-triazapentalenes are expected to change the fluorescence wavelength and intensity according to the hydrophobic environment in the cells.

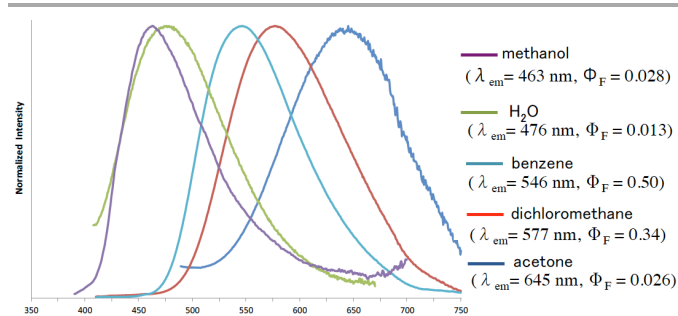


Figure 3. Emission behaviors and fluorescence spectra of **1e** in several solvents.

Next, we investigated the applicability of the long-wavelength fluorescent 1,3a,6a-triazapentalenes as fluorescent probes in a biological system. Since the di-cyano analog **1f** was not very stable against UV irradiation and its Φ_F was lower ($\Phi_F = 0.096$) than **1e** ($\Phi_F = 0.34$),¹⁷ mono-cyano analog **1e** was adopted for this purpose. Thus, HeLa cells were treated with a solution of **1e** (10 μM in 0.02% DMSO)²⁰ and monitored in the 572–642 nm wavelength region. As shown in Figure 4, the

fluorescent staining of HeLa cells was successfully observed without washing the cellular medium. The living HeLa cells were clearly visualized under fluorescence microscope observation, whereas the interiors of the control cells, which were treated with DMSO, were not stained. Since active uptake of fluorescent **1e** by living cells and fluorescence solvatochromism of **1e** enhance the fluorescence contrast between the cells and background, it was not necessary to fix the cells. Furthermore, cytotoxicity for the cells was not found over the observation period, suggesting that triazapentalene is suitable for connecting to small biofunctional molecules as fluorescence labels. This is the first experimental evidence that the 1,3a,6a-triazapentalene is applicable to the life science field as a fluorescence reagent. The further detailed investigation such as localization and quantitative analysis of **1e** inside cells are currently underway in our laboratory.

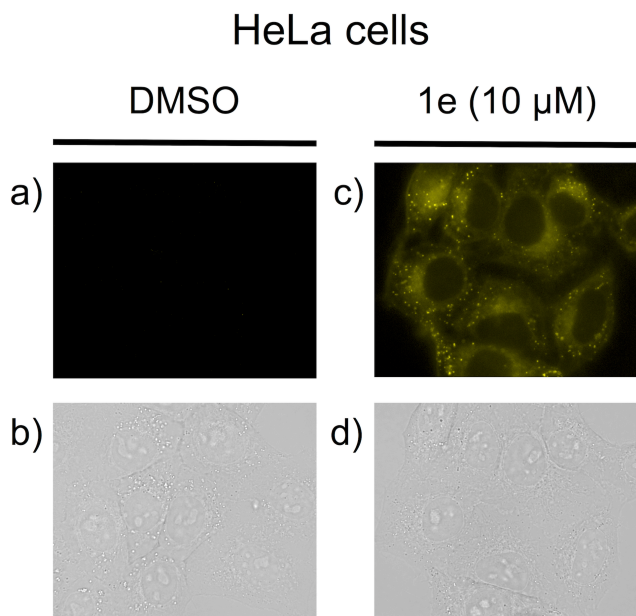
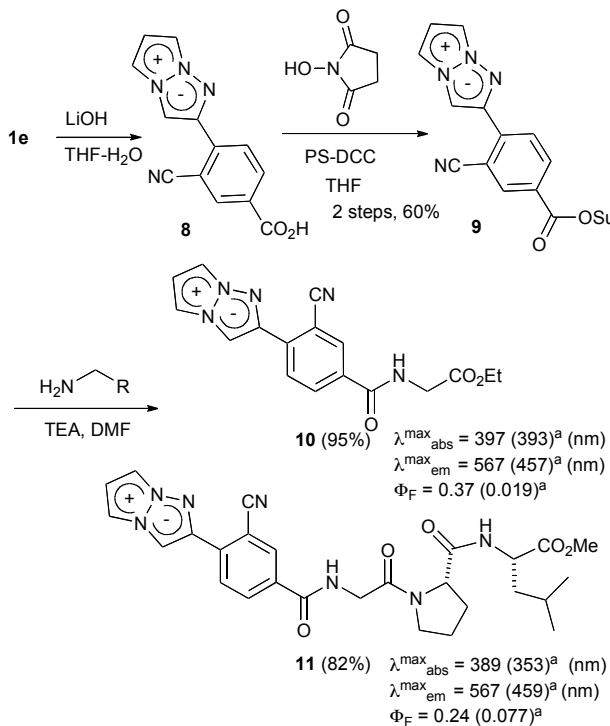


Figure 4 Observation of **1e** in HeLa cells. Living cells were cultured in 0.02% DMSO as a control (a and b) or with 10 μ M **1e** in 0.02% DMSO (c and d). Uptake of **1e** was monitored by using a fluorescence microscope (BZ-9000; Keyence) in a bright-field image (b and d) or in a fluorescence image with a BZ set (FF01-452/45 nm exciter, FF01-607/70 nm emitter, FF511 nn-Di01 dichroic mirror) (a and c).

The actual fluorescence observation of **1e** inside cells encouraged us to develop **1e** as a fluorescent labeling reagent. Thus, the conversion of the methyl ester moiety into *N*-hydroxy succinimide ester as a binding site was attempted. Treatment of **1e** with 1.2 equiv of lithium hydroxide afforded carboxylic acid **8**, which was directly used for the next condensation reaction. However, although the condensing reaction proceeded smoothly, the removal of the urea analogs generated from the condensing reagent was not straightforward due to the instability of the succinimide moiety of **9**. Finally, polymer-supported DCC was adopted as a useful condensing reagent to remove the urea by filtration, and the subsequent recrystallization gave the purified **9** in 60% two-step yield.

Having prepared the fluorescent labeling reagent **9**, the introduction of **9** into amino acids was examined (Scheme 3). Treatment of **9** with glycine ethyl ester in DMF afforded labeled glycine **10** in 95% yield. The fluorescence-labeled **10** exhibited yellow emission ($\lambda_{\text{em}}^{\text{max}} = 567$ nm) with a high quantum yield ($\Phi_F = 0.37$)¹⁷ in deaerated dichloromethane. Furthermore, the introduction of tri-peptide Gly-Pro-Leu was also examined, and the labeled tri-peptide **11** was obtained in 82% yield. The fluorescence observation of **11** showed the fluorescence maximum at 567 nm and acceptable fluorescent quantum yield ($\Phi_F = 0.24$)¹⁷ in deaerated dichloromethane. Therefore, the expansion of 1,3a,6a-triazapentalene to the compact fluorescent labeling reagent emitting yellow-red light was achieved. Furthermore, although the labelled glycine **10** and tri-peptide **11** were dissolved well in an organic solvent,²¹ their fluorescence properties in water were also measured. Since the emission maxima of **10** and **11** shifted to shorter wavelengths with similar absorption maximum, the Stokes shifts became small in water as is the case **1e**. The fluorescent quantum yields (Φ_F) were also reduced to 0.019 (**12**) and 0.077 (**13**).¹⁷ These changes in the fluorescence properties according to the polarity of environment might be useful as a fluorescent probe *in vivo* measurements.



Scheme 3 Synthesis of Fluorescent Labeling Reagent **11** and Its Application to the Amino Acids. ^ameasured in water.

Theoretical Investigation of the Optical Properties of 1,3a,6a-Triazapentalenes

In our preliminary communication, we first reported that the 1,3a,6a-triazapentalene skeleton without an additional fused ring system is a compact and highly fluorescent chromophore.

However, the detailed mechanisms of the fluorescence have not yet been elucidated. In this work, quantum chemical calculations were performed to investigate the optical properties of 1,3a,6a-triazapentalenes. Most of the theoretical calculations for the optical properties of dye molecules utilize the time-dependent density functional theory (TD-DFT), but in this work the high-level wavefunction-based approach using the complete active space second-order perturbation theory (CASPT2) method are also employed to provide a more reliable description of the excitation energies. The following synthetic 1,3a,6a-triazapentalenes were examined as the model substrates in this investigation: unsubstituted 1,3a,6a-triazapentalene **1a** as a basic structure, 2-(4-cyano)phenyl derivative **1b** as a standard analog in the previous communication, and synthetic **1g**, **1e**, and **1f** in this article.

Computational Details

The equilibrium geometry in the electronic ground state (S_0) is determined by the density functional theory (DFT) calculations using the B3LYP functionals, while the geometry optimization in the lowest $\pi\pi^*$ excited state $S_1(\pi\pi^*)$ is performed by the time-dependent DFT (TD-DFT) calculations employing the coulomb attenuated B3LYP (CAM-B3LYP) functionals.²² The C_s symmetry constraint is imposed for **1a**, **1b**, **1g**, and **1e**, while no constraint is applied for **1f** because the twisted structure is more stable due to the steric hindrance. The employment of the CAM-B3LYP functionals is due to the significant charge-transfer character involved in excitation to the S_1 state. The 6-31+G(d,p) basis set is used in the DFT calculations and the equilibrium geometries are determined both in the gas phase and in dichloromethane. The solvent effects are taken into account by the polarizable continuum solvation model (PCM)²³, where the radii are taken from the UFF force field.²⁴ After the geometry optimization, the vertical excitation and fluorescence energies are calculated at the S_0 and S_1 equilibrium structures (denoted as $(S_0)_{\text{min}}$ and $(S_1)_{\text{min}}$), respectively, by the TD-DFT(CAM-B3LYP) method. In PCM calculations, the linear-response method with a non-equilibrium solvation is employed to obtain the vertical excitation energies at $(S_0)_{\text{min}}$, while equilibrium solvation is adapted for calculation of the excitation energies during the S_1 geometry optimization.

The excitation energy is also refined at the DFT-optimized geometries by the CASPT2²⁵ method in order to obtain more reliable excitation energies. A level shift with a value of 0.3 is applied for the CASPT2 calculations.²⁶ The notation of CASPT2(m,n) is occasionally used, in which case the active space for a reference state-averaged complete active space self-consistent field (SA-CASSCF) wavefunction is composed of m electrons and n orbitals (SA-CASSCF(m,n)). The augmented correlation-consistent polarized double-zeta basis set (denoted as aug-cc-pVDZ) is employed in the CASPT2 calculations. In obtaining the oscillator strengths, the vertical excitation energies by CASPT2 and transition dipole moments by SA-CASSCF are used.

For **1a**, the active space for the reference SA-CASSCF wavefunction is comprised of six π orbitals (four π orbitals are doubly-occupied and two are unoccupied in the closed-shell configuration), and therefore it is denoted as SA-CASSCF(8,6). **1a** possesses ten π orbitals and the lowest and highest π orbitals are excluded from the active space. This is justified by the larger active space calculation, which includes all π orbitals (which corresponds to SA-CASSCF(10,8), and the active orbitals at $(S_0)_{\text{min}}$ are shown in the Supporting Information as Figure S1), where only a difference of ~ 0.01 eV is observed in the S_1 vertical excitation energies. The active space for other chromophores is composed of twelve electrons distributed in ten π orbitals (SA-CASSCF(12,10)), and the active orbitals of **1b** at $(S_0)_{\text{min}}$ are shown in Figure S2. As seen in the figure, the active space of the SA-CASSCF(12,10) wavefunction includes orbitals that correspond to the active orbitals of SA-CASSCF(8,6) in **1a**. For all chromophores, the S_0 and S_1 states are averaged with equal weights in the SA-CASSCF calculations, except where otherwise noted.

The DFT and TD-DFT calculations are performed using the Gaussian09 program package²⁷ while the CASPT2 calculations are carried out by the MOLPRO2010.1 program package.²⁸

Results and Discussion on the Optical Properties

We begin by investigating character of excited states of **1a** and **1b** at $(S_0)_{\text{min}}$ in the gas phase, followed by results and discussion on the optical properties of other chromophores in the gas phase and in dichloromethane.

1. Simple 1,3a,6a-triazapentalene (**1a**)

The S_0 and S_1 equilibrium structures of **1a** in the gas phase are shown in Figure 5, along with the bond lengths and atomic numbering (note that this numbering is different from the previous sections and is only used in the theoretical section). The significant geometrical changes upon photo-excitation involve the bond elongation of N3-C6 (1.370 \rightarrow 1.411 Å) and N1-N2 (1.344 \rightarrow 1.376 Å).

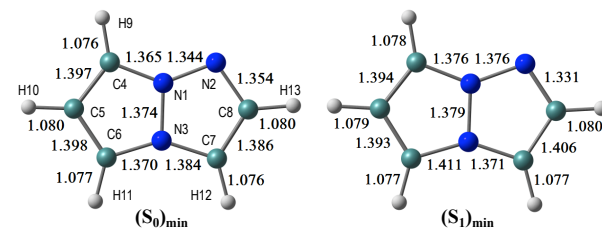


Figure 5 Equilibrium structures of **1a** in the S_0 and S_1 states in the gas phase. Bond lengths are given in units of Å.

The vertical excitation energies to the low-energy-lying $\pi\pi^*$ states are shown in Table 3, where in the CASPT2 calculation the S_0 and lowest three $\pi\pi^*$ states are averaged with equal weights in the reference SA-CASSCF(8,6) wavefunction. It is noted that, although a couple of $n\pi^*$ states are found between these $\pi\pi^*$ states in TD-DFT calculations, it is confirmed that the lowest-energy singlet excited-state is characterized by $\pi\pi^*$.

excitation, and therefore only the $\pi\pi^*$ states are examined in this investigation. The lowest $\pi\pi^*$ excited-state $S_1(\pi\pi^*)$ is viewed as the HOMO-LUMO transition (see the natural orbitals in Figure S1 (Supporting Information) and the CASPT2 excitation energy of 4.33 eV (286 nm) is in good agreement with the experimental value of 4.31 eV (288 nm), although the experimental measurements are performed in dichloromethane. The second $\pi\pi^*$ excited state is characterized by the HOMO \rightarrow LUMO+1 transition, and it lies close to the first $\pi\pi^*$ state in the CASPT2 calculation. The natural charges of the S_0 and S_1 states at $(S_0)_{\min}$ and their differences are shown in Figure S3.

Table 3 Vertical Excitation Energies (ΔE in eV and nm) and Oscillator Strengths (f in a.u.) of **1a** for the Low-Lying $\pi\pi^*$ States at $(S_0)_{\min}$.

State	TD-DFT (CAM-B3LYP)			CASPT2				
	ΔE (eV)	ΔE (nm)	f	Transition n	ΔE (eV)	ΔE (nm)	f	Transition n
1	4.79	259	0.262	$5\pi \rightarrow 1\pi^*$	4.33	286	0.213	$5\pi \rightarrow 1\pi^*$
2	5.33	232	0.052	$5\pi \rightarrow 2\pi^*$	4.43	280	0.250	$5\pi \rightarrow 2\pi^*$
3	5.49	225	0.010	$5\pi \rightarrow 3\pi^*$	5.53	224	0.384	$4\pi \rightarrow 1\pi^*$

The main orbital transition is also shown.

2. 2-(4-cyano)phenyl-1,3a,6a-triazapentalene (**1b**)

The S_0 and S_1 equilibrium structures of **1b** in the gas phase are shown in Figure 6, along with the bond lengths and atomic numbering. The transition to the S_1 state involves the bond elongation of C7-C8 (1.394 \rightarrow 1.444 Å) and shortening of the central C8-C13 bond (1.469 \rightarrow 1.421 Å).

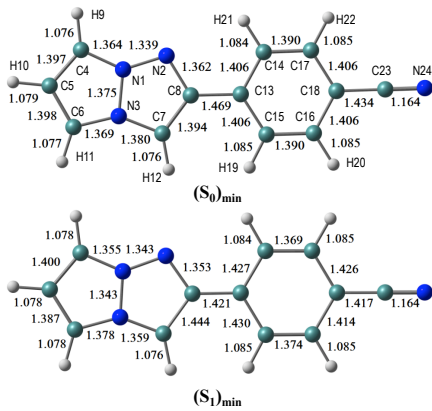


Figure 6 Equilibrium structures of **1b** in the S_0 and S_1 states in the gas phase. Bond lengths are given in units of Å.

The vertical excitation energies to the low-energy-lying $\pi\pi^*$ states are shown in Table 4. In the CASPT2 calculation, the S_0 and lowest three $\pi\pi^*$ states are averaged with equal weights in the reference SA-CASSCF(12,10) wavefunction. The vertical excitation energies to the $S_1(\pi\pi^*)$ state are 3.85 (322 nm) and 3.25 eV (381 nm) for the TD-DFT and CASPT2 calculations, respectively, and the CASPT2 excitation energy is in remarkably good agreement with the experimental value of 3.25 eV (381 nm) (note again that the experimental measurements are performed in dichloromethane). Excitation to the S_1 state is characterized by the HOMO \rightarrow LUMO transition (see Figure 7 and also Figure S2), and as expected

from the shape of the two relevant orbitals, the S_1 transition involves charge transfer from the 1,3a,6a-triazapentalene skeleton to the substituted phenyl ring. This is clearly seen from the large dipole moment in the S_1 state (19.47 debye) compared to that of the S_0 state (7.11 debye) at $(S_0)_{\min}$ (see Table S1). The charge-transfer character of S_1 is also recognized by the natural charges, where the sums of the natural charges in the 1,3a,6a-triazapentalene skeleton (atoms from N1 to H12) are 0.022 and 0.542 in the S_0 and S_1 states, respectively (see also Table S1). Since the S_1 state exhibits a charge-transfer character, it may be possible to observe the twisted intramolecular charge transfer (TICT) state involving the rotation of the phenyl ring around the central C8-C13 bond. In order to check this, we performed frequency analysis at $(S_1)_{\min}$ and confirmed that the planar geometry is the minimum energy structure in the S_1 state.

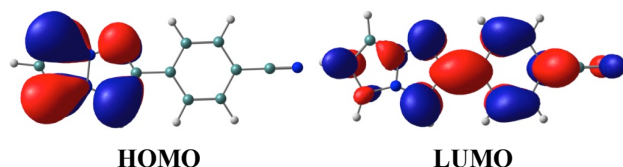


Figure 7 Natural orbitals of **1b** involved in the excitation to the S_1 state.

As seen in Table 4, the second and third $\pi\pi^*$ states can be described as a mixing of two configurations, HOMO \rightarrow LUMO+1 ($9\pi \rightarrow 2\pi^*$) and HOMO-1 \rightarrow LUMO ($8\pi \rightarrow 1\pi^*$). It is noted that the HOMO \rightarrow LUMO+1 ($9\pi \rightarrow 2\pi^*$) transition corresponds to $S_0 - S_1$ excitation of **1a**, while the $S_0 - S_1$ transition of **1b** corresponds to excitation to the second $\pi\pi^*$ state of **1a** (see the natural orbitals given in Figure S1 and Figure S2). Therefore, the electronic character of the S_1 state is different between **1a** and **1b**.

Table 4 Vertical Excitation Energies (ΔE in eV and nm) and Oscillator Strengths (f in a.u.) of **1b** for the Low-Energy-Lying $\pi\pi^*$ States at $(S_0)_{\min}$.

State	TD-DFT (CAM-B3LYP)			CASPT2				
	ΔE (eV)	ΔE (nm)	f	Transition	ΔE (eV)	ΔE (nm)	f	Transition
1	3.85	322	0.083	$9\pi \rightarrow 1\pi^*$	3.25	381	0.047	$9\pi \rightarrow 1\pi^*$
2	4.67	266	0.043	$9\pi \rightarrow 2\pi^*$, $8\pi \rightarrow 1\pi^*$	3.89	319	0.755	$9\pi \rightarrow 2\pi^*$, $8\pi \rightarrow 1\pi^*$
3	4.80	258	1.111	$9\pi \rightarrow 2\pi^*$, $8\pi \rightarrow 1\pi^*$	4.17	298	0.012	$9\pi \rightarrow 2\pi^*$, $8\pi \rightarrow 1\pi^*$

The main orbital transition is also shown.

3. Green fluorescence (**1g**), yellow fluorescence (**1e**), and red fluorescence (**1f**) derivatives and comparison with the experimental results

The optimized structures of **1f** in the S_0 and S_1 states are shown in Figure 8, where the dihedral angle of $d(C7-C8-C13-C15)$ representing twisting of the phenyl ring around the central C8-C13 atoms is 40.6 degrees at $(S_0)_{\min}$, and slightly decreases to 29.7 degrees at $(S_1)_{\min}$. The other chromophores (**1g** and **1e**) maintain the planar geometry and the Cartesian coordinates of

the optimized structures are given in the Supporting Information.

Excitation to the S_1 state involves the HOMO \rightarrow LUMO transition, and all chromophores (**1g**, **1e**, and **1f**) exhibit the same charge-transfer character. The vertical excitation and fluorescence energies are summarized in Table 5. We note here that in this table a slight discrepancy is found in the $S_1(\pi\pi^*)$ vertical excitation energies of CASPT2 for **1a** and **1b** with respect to the values shown in Table 3 and Table 4, since in Table 5 only the S_0 and S_1 states are averaged with equal weights in the reference SA-CASSCF wavefunction.

The CASPT2 calculations are performed only in the gas phase, and therefore we estimate the excitation energies in dichloromethane using the solvatochromic shifts of TD-DFT calculations (the estimated values are shown in parenthesis). Figure 9 shows the comparison of absorption and fluorescence wavelengths between the theoretical calculations and experimental results. Although the calculated fluorescence wavelengths are shorter than the experimental values, the figure clearly demonstrates a good correlation between the two values. The overestimation of the fluorescence energies may be attributable to the insufficient treatment of the solvent environments, because excitation involves a significant charge-transfer character. The explicit treatment of the solvent

molecules in the framework of the QM/MM approach or the state-specific approach^{29,30} would be appropriate for a more quantitative description of the fluorescence energies.

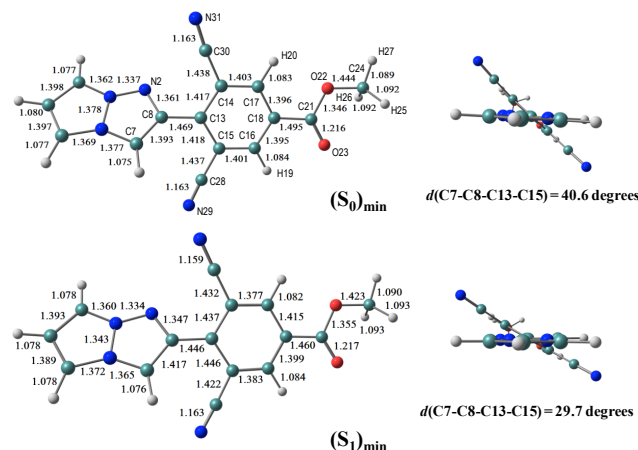


Figure 8 Equilibrium structures of **1f** in the S_0 and S_1 states in the gas phase. Bond lengths are given in units of Å.

Table 5 Vertical Excitation Energies (ΔE in eV and nm) and Oscillator Strengths (f in a.u.) for the S_1 State Calculated by TD-DFT and CASPT2 at (S_0)_{min}.

	TD-DFT (in gas)			TD-DFT (in dichloromethane)			CASPT2 (in gas)			exp.	
	ΔE (eV)	ΔE (nm)	f	ΔE (eV)	ΔE (nm)	f	ΔE (eV)	ΔE (nm)	f	ΔE (nm)	
1a	4.79	259	0.262	4.62	268	0.276	4.26	291 (300) ^a	0.351	288	
1b	3.85	322	0.083	3.66	339	0.143	3.26	380 (397)	0.058	381	
1g	3.91	317	0.096	3.73	332	0.159	3.32	374 (389)	0.057	376	
1e	3.51	353	0.048	3.33	372	0.076	2.97	418 (437)	0.051	420	
1f	3.21	387	0.033	3.11	398	0.050	2.76	450 (461)	0.040	466	

^aThe number in parenthesis is an estimate in dichloromethane.

Table 6 Vertical Fluorescence Energies (ΔE in eV and nm) and Oscillator Strengths (f in a.u.) for the S_1 State Calculated by TD-DFT and CASPT2 at (S_1)_{min}.

	TD-DFT (in gas)			TD-DFT (in dichloromethane)			CASPT2 (in gas)			exp.	
	ΔE (eV)	ΔE (nm)	f	ΔE (eV)	ΔE (nm)	f	ΔE (eV)	ΔE (nm)	f	ΔE (nm)	
1a	4.62	268	0.276	4.33	287	0.446	4.04	307 (326) ^a	0.382	389	
1b	3.46	358	0.137	3.18	390	0.345	2.88	430 (462)	0.092	509	
1g	3.48	356	0.164	3.19	389	0.372	2.91	426 (459)	0.101	510	
1e	3.14	394	0.072	2.91	425	0.191	2.63	471 (502)	0.078	572	
1f	2.82	440	0.046	2.68	463	0.134	2.33	533 (556)	0.060	632	

^aThe number in parenthesis is an estimate in dichloromethane.

In the Supporting Information (Table S1 and S2), the sums of the natural charges in the 1,3a,6a-triazapentalene skeleton and dipole moments in the S_0 and S_1 states at $(S_0)_{\min}$ and $(S_1)_{\min}$ are given for all chromophores. It is noteworthy that there is a clear correlation between the wavelengths and the natural charges (also dipole moments) in the S_1 state, where a larger charge separation induces longer absorption and fluorescence wavelengths. It is also noted that the absorption and fluorescence wavelengths are longer in dichloromethane than in the gas phase because the charge-transfer state is more stabilized in polar solvents.

Finally, we comment that the CASPT2 method is more reliable than the TD-DFT approach, but the computational cost is much more expensive. As seen in the present work, the TD-DFT method predicts slightly higher excitation energies than those by CASPT2, but the correlation with experimental results is surprisingly good. Therefore, for chromophores of larger size, where CASPT2 calculations are prohibitive, the TD-DFT method can be reliably used to predict the optical properties of 1,3a,6a-triazapentalenes.

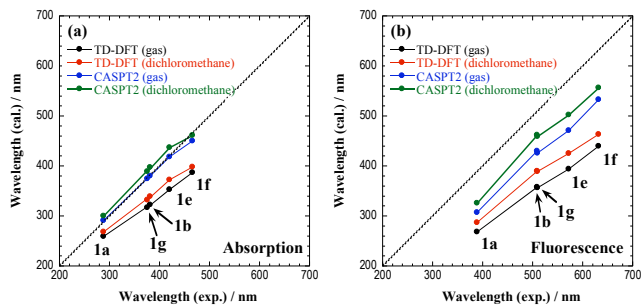


Figure 9 Comparison of (a) absorption and (b) fluorescence wavelengths between the theoretical calculations and experimental results. The central line indicates a perfect theory/experiment match.

Conclusions

The fluorescence wavelengths of 1,3a,6a-triazapentalenes were extended to the red color region. Based on the noteworthy correlation of the fluorescence wavelength with the inductive effect of the 2-substituent, further electron deficient 2-(2-cyano-4-methoxycarbonylphenyl)-1,3a,6a-triazapentalene and 2-(2,6-dicyano-4-methoxycarbonylphenyl)-1,3a,6a-triazapentalene were synthesized. They exhibited yellow and red fluorescence and large Stokes shift respectively, and the 1,3a,6a-triazapentalene system enables the same fluorescent chromophore to cover the entire region of visible wavelengths. The potential applications of the 1,3a,6a-triazapentalene system as fluorescent probes to the fields of the life sciences were investigated, and the 1,3a,6a-triazapentalene system was clearly proven to be useful as a fluorescent reagent for living cells. The *N*-hydroxysuccinimide ester derivative of yellow fluorescent 1,3a,6a-triazapentalene as a compact labeling reagent was confirmed to readily label the amino group. Finally, quantum chemical calculations were performed to investigate the optical properties of 1,3a,6a-triazapentalenes. These calculations revealed that excitation involves significant charge-transfer from the 1,3a,6a-triazapentalene skeleton to the 2-substituent. The calculated absorption and fluorescence

wavelengths showed a good correlation with the experimental ones, which allows us to design substituents that exhibit the desired optical properties.

Acknowledgements

We thank professors Kazuki Sada and Kenta Kokado for the TGA analysis of **2**. This work was partially supported by Grant-in-Aid for Scientific Research (Grant No. 24310162), and Grant-in-Aid for Scientific Research on Innovative Areas (Project No. 2301: Chemical Biology of Natural Products) from the Ministry of Education, Culture, Sports, Science, and Technology, Japan. K. N. is grateful to the Naito Foundation and Yamada Foundation for support through a Research Fund for Recently Independent Professor. A. O. is grateful to JSPS for a Research Fellowship (No. 26-2457) for Young Scientists.

Notes and references

^a Department of Pharmaceutical Science, The University of Tokushima, 1-78 Shomachi, Tokushima 770-8505, Japan.

^b Graduate School of Chemical Sciences and Engineering, Hokkaido University, Sapporo 060-0810, Japan

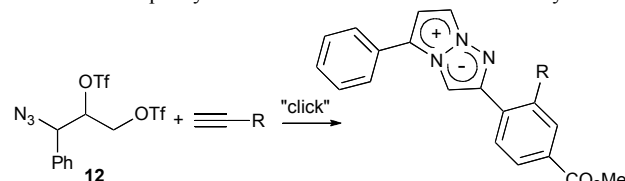
^c Department of Chemistry, Faculty of Science, Hokkaido University, Kita-ku, Sapporo 060-0810, Japan

^d Catalysis Research Center, Hokkaido University, Sapporo 001-0021, Japan

† Electronic Supplementary Information (ESI) available: Experimental details for synthesis of triazapentalenes and fluorescent cell staining, absorption and fluorescence spectra, and ¹H and ¹³C NMR spectra. Molecular orbitals, natural charges, dipole moments, and Cartesian coordinates of triazapentalenes (**1a**, **1b**, **1g**, **1e**, and **1f**). See DOI: 10.1039/b0000000x/

- 1 (a) J. Shinar, Ed. *Organic Light-Emitting Devices*, Springer, New York, 2004. (b) B. Valeur, *Molecular Fluorescence*, WILEY-VCH, Weinheim, 2002. (c) R. K. Willardson, E. Weber, G. Mueller, Y. Sato, *Electroluminescence I, Semiconductors and Semimetals Series*, Academic Press, New York, **1999**.
- 2 For selected recent examples of fluorescent molecule: (a) M. Shimizu, M. Takeda, M. Higashi and T. Hiyama, *Angew. Chem. Int. Ed.*, 2009, **48**, 3653-3656; (b) A. Lorbach, M. Molte, H. Li, H.-W. Lerner, M. C. Holthausen, F. Jäkle and M. Wagner, *Angew. Chem. Int. Ed.*, 2009, **48**, 4584-4588; (c) L. G. Mercier, W. E. Piers, and M. Parvez, *Angew. Chem. Int. Ed.*, 2009, **48**, 6108-6111; (d) Z. Zhao, Z. Wang, P. Lu, Y. K. Chan, D. Liu, J. W. Y. Lam, H. H. Y. Sung, I. D. Williams, Y. Ma and B. Z. Tang, *Angew. Chem. Int. Ed.*, 2009, **48**, 7608-7611; (e) A. Caruso Jr., M. A. Siegler and J. D. Tovar, *Angew. Chem. Int. Ed.*, 2010, **49**, 4213-4217; (f) Y. Ren and T. Baumgartner, *J. Am. Chem. Soc.* 2011, **133**, 1328-1340; (g) A. R. Siamaki, M. Sakalauskas and B. A. Arndtsen, *Angew. Chem. Int. Ed.*, 2011, **50**, 6552-6556; (h) Z. Zhang, B. Xu, J. Su, L. Shen, Y. Xie and H. Tian, *Angew. Chem. Int. Ed.*, 2011, **50**, 11654-11657; (i) D. Zhao, J. Hu, N. Wu, X. Huang, X. Qin, J. Lan and J. You, *Org. Lett.* 2011, **13**, 6516-6519; (j) B. Liu, Z. Wang, N. Wu, M. Li, J. You and J. Lan, *Chem. Eur. J.* 2012, **18**, 1599-1603; (k) S. Matsumoto, H. Abe and M. Akazome, *J. Org. Chem.* 2013, **78**, 2397-2404; (l) T. Mutai, H. Sawatani, T. Shida, H. Shono and K. Araki, *J. Org. Chem.* 2013, **78**, 2482-2489; (m) L.

- Zilbershtein-Shklanovsky, M. Weitman, D. T. Major and B. Fischer, *J. Org. Chem.* 2013, **78**, 11999-12008.
- 3 For books and recent review; see, (a) M. Ueda, *Chem. Lett.* 2012, **41**, 658-666, and references are therein. (b) J. Shinar, Ed. *Organic Light-Emitting Devices*, Springer, New York, (2004); (c) B. Valeur, *Molecular Fluorescence*, WILEY-VCH, Weinheim, (2002); (d) R. K. Willardson, E. Weber, G. Mueller, Y. Sato, *Electroluminescence I, Semiconductors and Semimetals Series*, Academic Press, New York, (1999).
- 4 K. Namba, A. Osawa, S. Ishizaka, N. Kitamura, N and K. Tanino, *J. Am. Chem. Soc.* 2011, **133**, 11466-11469.
- 5 The computational structural study of unsubstituted 1,3a,6a-triazapentalene **1a**: see C. Carra, T. Bally, T. A. Jenny and A. Albini, *Photochem. Photobiol. Sci.*, 2002, **1**, 38-44.
- 6 The photodecomposition of benzotriazapentalenes as an aryl fused system exhibit very little fluorescence ($\Phi_F = 0.0001$): see A. Albini, A. G. Bettinetti and G. Minoli, *J. Am. Chem. Soc.* 1991, **113**, 6928-6934.
- 7 Synthesis of 1,3a,6a-triazapentalene derivatives with aryl fused and heteroaryl fused systems: see (a) O. Tsuge and H. Samura, *Chem. Lett.* 1973, 175-180; (b) J. H. Lee, A. Matsumoto, M. Yoshida and O. Simamura, *Chem. Lett.* 1974, 951-954; (c) I. M. McRobbie, O. Meth-Cohn and H. Suschitzky, *Tetrahedron Lett.* 1976, **12**, 925-928; (d) A. Albini, G. F. Bettinetti and G. Minoli, *Chem. Lett.* 1981, 331-334; (e) A. Albini, G. F. Bettinetti and G. Minoli, *J. Org. Chem.* 1983, **48**, 1080-1083. (f) A. Albini, G. F. Bettinetti and G. Minoli, *J. Am. Chem. Soc.* 1991, **113**, 6928-6934; (g) A. Albini, G. Bettinetti, and G. Minoli, *J. Am. Chem. Soc.* 1997, **119**, 7308-7315; (h) A. Albini, G. Bettinetti and G. Minoli, *J. Am. Chem. Soc.* 1999, **121**, 3104-3113; (i) T. Kim, K. Kim and Y. J. Park, *Eur. J. Org. Chem.* 2002, 493-502; (j) Y.-A. Choi, K. Kim and Y. J. Park, *Tetrahedron Lett.* 2003, **44**, 7506-7511; (k) C. Nyffenegger, E. Pasquinet, F. Suzenet, D. Poullain, C. Jarry, J.-M. Léger and C. Guillaumet, *Tetrahedron Lett.* 2008, **64**, 9567-9573. (l) C. Nyffenegger, E. Pasquinet, F. Suzenet, D. Poullain and G. Guillaumet, *Synlett*, 2009, 1318-1320.
- 8 Synthesis of 1,3a,6a-triazapentalenes without an additional fused ring system by other groups: see (a) H. Koga, M. Hirobe and T. Okamoto, *Tetrahedron Lett.* 1978, **19**, 1291-1294; (b) Y. Chen, D. Wang, J. L. Petersen, N. G. Akhmedov and X. Shi, *Chem. Commun.* 2010, **46**, 6147-6149. (c) R. Cai, D. Wang, Y. Chen, W. Yan, N. R. Geise, S. Sharma, H. Li, J. L. Petersen, M. Li, X. Shi. *Chem. Commun.*, 2014, **50**, 7303-7305.
- 9 K. Namba, A. Mera, A. Osawa, E. Sakuda, N. Kitamura and K. Tanino, *Org. Lett.* 2012, **14**, 5554-5557.
- 10 For large Stokes Shift dyes, see (a) J. R. Lakowicz, Principles of Fluorescence Spectroscopy, 3rd ed.; Springer: New York, 2006. For selected recent examples (b) S. Rihm, P. Retailleau, A. D. Nicola, G. Ulrich, and R. Ziessel, *J. Org. Chem.* 2012, **77**, 8851-8863; (c) A. C. Benniston, T. P. L. Winstanley, H. Lemmetyinen, N. V. Tkachenko, R. W. Harrington, C. Wills, *Org. Lett.* 2012, **14**, 1374-1377; (d) J. F. Areneda, W. E. Piers, B. Heyne, R. McDonald, *Angew. Chem., Int. Ed.* 2011, **50**, 12214-12217, and references are therein.
- 11 For emission tunable fluorophores, see (a) A.P. Demchenko, Advanced Fluorescence Reporters in Chemistry and Biology I, Springer, Berlin, **2010**; (b) E. J. Choi, E. Kim, Y. Lee, A. Jo and S. B. Park, *Angew. Chem. Int. Ed.* 2014, **53**, 1346-1350; (b) E. Kim, M. Koh, J. Ryu and S. B. Park, *J. Am. Chem. Soc.* 2008, **130**, 12206-12207; (c) L. D. Lavis, R. T. Raines, *ACS. Chem. Biol.*, 2008, **3**, 142-155.
- For quantum yields tunable fluorophores, see (a) T. Miura, Y. Urano, K. Tanaka, T. Nagano, K. Ohkubo and S. Fukuzumi, *J. Am. Chem. Soc.* 2003, **125**, 8666-8671; (b) T. Ueno, Y. Urano, K. Setsukinai, H. Tkakusa, H. Kojima, K. Kikuchi, K. Ohkubo, S. Fukuzumi and T. Nagano, *J. Am. Chem. Soc.* 2004, **126**, 14079-14085; (c) Y. Urano, M. Kamiya, K. Kanda, T. Ueno, K. Hirose and T. Nagano, *J. Am. Chem. Soc.* 2005, **127**, 4888-4894; (d) T. Ueno, Y. Urano, H. Kojima and T. Nagano, *J. Am. Chem. Soc.* 2006, **128**, 10640-10641.
- 12 M. S. Goncalves, *Chem. Rev.* 2009, **109**, 190-212.
- 13 Fluorescence quantum yields were estimated by using 9,10-diphenylanthracene (9,10-DPA) in cyclohexane ($\Phi_F = 0.91$) as a standard.
- 14 Although the use of trimethylsilylacetylene also gave the coupling product, TMS group was cleaved under the condition of next CO insertion reaction.
- 15 S. Ullrich, Z. Nazir, A. Büsing, U. Scheffer, D. Wirth, J. W. Bats, G. Dürner and M. W. Göbel, *ChemBioChem* 2011, **12**, 1223-1229.
- 16 Other palladium source and ligand such as Pd(acac)₂, Pd(OAc)₂, Pd(OCOCF₃)₂, PdCl₂(CH₃CN)₂, PdCl₂(PhCN)₂, Pd(PPh₃)₄, Pd₂(dba)₃, P(t-Bu)₃, dpfp, Xantphos, P(O*i*-Pr)₃, and P(*o*-tol)₃, gave **9** in trace to poor yield.
- 17 Fluorescence quantum yields were estimated by using rhodamine B in ethanol ($\Phi_F = 0.94$) as a standard.
- 18 (a) K. Nagy, E. Orbán, S. Bösze and P. Kele, *Chem. Asian J.* 2010, **5**, 773-777; (b) A. Martin, C. Long, R. J. Forster, T. E. Keyes, *Chem. Commun.* 2012, **48**, 5617-5619; (c) G. B. Cserep, K. N. Enyedi, A. Demeter, G. Mező and P. Kele, *Chem. Asian J.* 2013, **8**, 494-502.
- 19 The 4-phenyl analogues were readily obtained by the similar click reaction of 1-phenyl-substituted azidoditriflate **12** with alkynes.



R = H; 82%, $\lambda_{\text{max}}^{\text{abs}} = 345 \text{ nm}$ ($\epsilon = 22600$), $\lambda_{\text{max}}^{\text{em}} = 548 \text{ nm}$, $\Phi_F = 0.35$

R = CN; 88%, $\lambda_{\text{max}}^{\text{abs}} = 432 \text{ nm}$ ($\epsilon = 4560$), $\lambda_{\text{max}}^{\text{em}} = 613 \text{ nm}$, $\Phi_F = 0.07$

- 20 The fluorescence properties of **1e** in this solution (0.02% DMSO); $\lambda_{\text{max}}^{\text{abs}} = 340 \text{ nm}$, $\lambda_{\text{max}}^{\text{em}} = 485 \text{ nm}$, $\Phi_F = 0.035$
- 21 The lithium salt of **12** obtained by hydrolysis of methyl ester moiety (C-terminus) was readily dissolved in water. The fluorescent properties of lithium salt in water; $\lambda_{\text{max}}^{\text{abs}} = 390 \text{ nm}$, $\lambda_{\text{max}}^{\text{em}} = 524 \text{ nm}$, $\Phi_F = 0.0033$
- 22 T. Yanai, D. P. Tew and N. C. Handy, *Chem. Phys. Lett.* 2004, **393**, 51-57.
- 23 M. Cossi, G. Scalmani, N. Rega and V. Barone, *J. Chem. Phys.* 2002, **117**, 43-54.
- 24 A. K. Rappe, C. J. Casewit, K. S. Colwell, W. A. Goddard and W. M. Skiff, *J. Am. Chem. Soc.* 1992, **114**, 10024-10035.
- 25 P. Celani and H.-J. Werner, *J. Chem. Phys.* 2000, **112**, 5546-5557.
- 26 B. O. Roos and K. Andersson, *Chem. Phys. Lett.* 1995, **245**, 215-223.
- 27 Gaussian 09, Revision C.01, M. J. Frisch, G. W. Trucks, H. B. Schlegel, G. E. Scuseria, M. A. Robb, J. R. Cheeseman, G. Scalmani, V. Barone, B. Mennucci, G. A. Petersson, H. Nakatsuji, M. Caricato, X. Li, H. P. Hratchian, A. F. Izmaylov, J. Bloino, G. Zheng, J. L. Sonnenberg, M. Hada, M. Ehara, K. Toyota, R. Fukuda, J. Hasegawa, M. Ishida, T. Nakajima, Y. Honda, O. Kitao, H. Nakai, T. Vreven, J. A. Montgomery, J. E. Peralta, F. Ogliaro,

- M. Bearpark, J. J. Heyd, E. Brothers, K. N. Kudin, V. N. Staroverov, R. Kobayashi, J. Normand, K. Raghavachari, A. Rendell, J. C. Burant, S. S. Iyengar, J. Tomasi, M. Cossi, N. Rega, J. M. Millam, M. Klene, J. E. Knox, J. B. Cross, V. Bakken, C. Adamo, J. Jaramillo, R. Gomperts, R. E. Stratmann, O. Yazyev, A. J. Austin, R. Cammi, C. Pomelli, J. W. Ochterski, R. L. Martin, K. Morokuma, V. G. Zakrzewski, G. A. Voth, P. Salvador, J. J. Dannenberg, S. Dapprich, A. D. Daniels, Farkas, J. B. Foresman, J. V. Ortiz, J. Cioslowski and D. J. Fox.
- 28 MOLPRO, version 2010.1, a package of *ab initio* programs, H.-J. Werner, P. J. Knowles, G. Knizia, F. R. Manby, M. Schütz and others.
- 29 R. Improta, V. Barone, G. Scalmani and M. J. Frisch, *J. Chem. Phys.* 2006, **125**, 54103-54109.
- 30 R. Improta, G. Scalmani, M. J. Frisch and V. Barone, *J. Chem. Phys.* 2007, **127**, 74504-74509.